



Long-term sediment decline causes ongoing shrinkage of the Mekong megadelta, Vietnam

Toru Tamura, van Lap Nguyen, Thi Kim Oanh Ta, Mark Bateman, Marcello Gugliotta, Edward J. Anthony, Rei Nakashima, Yoshiki Saito

► To cite this version:

Toru Tamura, van Lap Nguyen, Thi Kim Oanh Ta, Mark Bateman, Marcello Gugliotta, et al.. Long-term sediment decline causes ongoing shrinkage of the Mekong megadelta, Vietnam. Scientific Reports, 2020, 10 (1), <10.1038/s41598-020-64630-z>. <hal-03146686>

HAL Id: hal-03146686

<https://hal.science/hal-03146686v1>

Submitted on 1 Mar 2021

HAL is a multi-disciplinary open access archive for the deposit and dissemination of scientific research documents, whether they are published or not. The documents may come from teaching and research institutions in France or abroad, or from public or private research centers.

L'archive ouverte pluridisciplinaire **HAL**, est destinée au dépôt et à la diffusion de documents scientifiques de niveau recherche, publiés ou non, émanant des établissements d'enseignement et de recherche français ou étrangers, des laboratoires publics ou privés.



Distributed under a Creative Commons CC BY 4.0 - Attribution - International License



OPEN

Long-term sediment decline causes ongoing shrinkage of the Mekong megadelta, Vietnam

Toru Tamura^{1,2}✉, Van Lap Nguyen³, Thi Kim Oanh Ta³, Mark D. Bateman⁴,
Marcello Gugliotta⁵, Edward J. Anthony^{6,7}, Rei Nakashima¹ & Yoshiki Saito^{1,5}

Since the 1990s the Mekong River delta has suffered a large decline in sediment supply causing coastal erosion, following catchment disturbance through hydropower dam construction and sand extraction. However, our new geological reconstruction of 2500-years of delta shoreline changes show that serious coastal erosion actually started much earlier. Data shows the sandy coast bounding river mouths accreted consistently at a rate of +2 to +4 km²/year. In contrast, we identified a variable accretion rate of the muddy deltaic protrusion at Camau; it was < +1 km²/year before 1400 years ago but increased drastically around 600 years ago, forming the entire Camau Peninsula. This high level of mud supply had sharply declined by the early 20th century after a vast canal network was built on the delta. Since then the Peninsula has been eroding, promoted by the conjunction of mud sequestration in the delta plain driven by expansion of rice cultivation, and hysteresis of long-term muddy sedimentation that left the protrusion exposed to wave erosion. Natural mitigation would require substantial increases in sediment supply well above the pre-1990s levels.

Coastal lowlands of river deltas, along with their usually humid climate, are characterized by high food productivity that supports large populations. They are also highly vulnerable to climate and sea-level changes as well as the impacts of human activities^{1–3}. The Mekong delta, southern Vietnam, is the third largest delta in the world and has been characterized by long-term large sediment supply in its extensive catchment under the influence of the rainy Asian monsoon climate. However, recent anthropogenic catchment disturbances such as upstream hydropower dam construction^{4,5} and fluvial sand mining^{6–9}, possibly along with climate change-induced discharge reduction¹⁰, are considered to have caused severe decline in the sediment discharge to the coast, compounding concerns raised by exacerbated subsidence due to accelerated groundwater extraction¹¹ and thus leading to alarms being raised regarding the increasing vulnerability of this populous megadelta. This declining sediment supply has led to enhanced coastal erosion with high-resolution satellite images from 1993 to 2013 indicating a substantial increase in the last 10 years¹². Longer-term analysis covering 1973–2015 also confirmed accelerated coastal erosion in the last few decades, particularly after 2005, in response to the increased capacity of hydropower dams in the Mekong's catchment¹³ and intensive sand mining in the deltaic channels^{6–9}.

While the fine-tuned characterization of the delta's recent shoreline changes has highlighted the impact of industrial activities within the Mekong catchment after the 1990s, a further question persists. The exacerbation of coastal erosion after the 1990s mainly concerned the sandy river mouth area of the delta. The muddy coast along the Camau Peninsula, which forms the bulk of the large Mekong delta protrusion into the East Sea (or South China Sea), has been eroding since the 1970s^{13,14}, with historical maps indicating that erosion may have started prior to 1940¹⁵. The ongoing shrinkage of the Mekong delta therefore cannot simply be attributed to the direct impact of recent industrial activities within the Mekong catchment. We contend that a long-term perspective using the sedimentary record is indispensable to understand the underlying causes of the Mekong delta's shrinkage.

Long-term shoreline changes of the Mekong delta have only been constrained in the river mouth area¹⁶ and relevant data have been missing in the southwestern delta protuberance, which has led previous studies to make assumptions on delta growth/erosion in this area^{17,18}. We hereby reconstruct the entirety of the East Sea shoreline

¹Geological Survey of Japan, AIST, Tsukuba, Ibaraki, 305-8567, Japan. ²Graduate School of Frontier Sciences, The University of Tokyo, Kashiwa, Chiba, 277-8561, Japan. ³HCMC Institute of Resources Geography, VAST, Ho Chi Minh City, Vietnam. ⁴Department of Geography, University of Sheffield, Sheffield, S10 2TN, UK. ⁵Estuary Research Center, Shimane University, Matsue, Shimane, 690-8504, Japan. ⁶Aix Marseille Univ, CNRS, IRD, INRA, Coll France, CEREGE, Aix-en-Provence, France. ⁷USR LEEISA, CNRS, Cayenne, French Guiana. ✉e-mail: toru.tamura@aist.go.jp

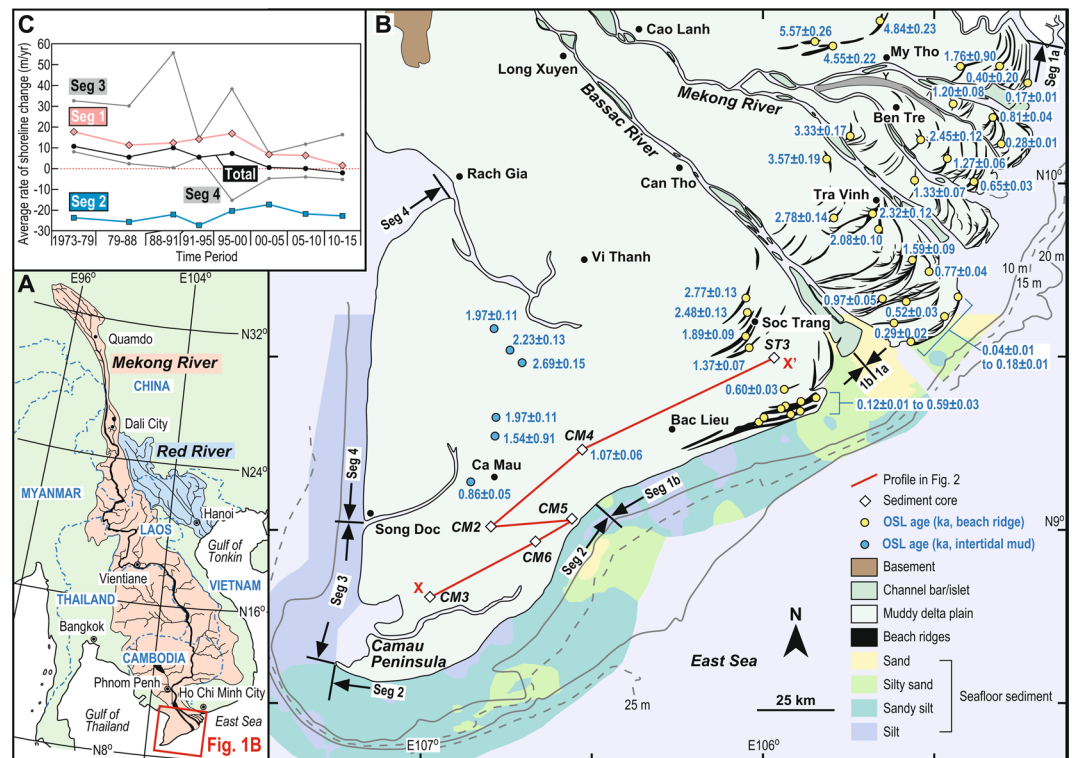


Figure 1. (A) Location of the Mekong River delta. Catchments of the Mekong and Red rivers are shaded. The map was derived from ref. ¹⁹ and generated with the software Adobe Illustrator 2020. (B) A map compiling geomorphology of the Mekong River delta⁴⁵ and bathymetry relative to mean sea level and substrate of the coastal area^{21,30}. A transect (X-X') is defined by linking six newly obtained drill cores for the cross section in Fig. 2. OSL ages NE and SW of the Bassac River are from existing¹⁶ and newly reported data in this paper, respectively. Shoreline segments are defined following previous spatial analysis¹³ while Seg 1 is further divided here into Segs 1a and 1b by the mouth of the Bassac River. The map was simplified from ref. ⁴⁵ and generated with the software Adobe Illustrator 2020. (C) Temporal variations of average rates of shoreline change from 1973 to 2015 for shoreline segments¹³.

of the Mekong delta by compiling newly obtained sediment and landform records with existing data. The reconstruction indicates temporal and spatial variations in shoreline change and highlights a close link between the onset of secular erosion and irrigation canal network development on the delta, compounded by hysteresis of the longer-term rapid muddy accretion.

Study Area

The Mekong delta has prograded over the last 8000 years in response to the deceleration of the post-glacial sea-level rise^{19,20} and is a representative of a mixed-energy delta^{21,22}. At present, tide-modulated wave processes dominate the open coast^{22,23}, whereas distributary channels are characterized by an upstream to downstream transition from fluvial to tide-dominated estuarine processes^{24–26}. Contrasts between the winter and summer monsoons define an annual sedimentary cycle on the coast^{23,27,28}. The southwesterly summer monsoon is characterised by a weaker wind and wave regime but brings moisture that causes river flooding and fluvial sediment supply, whereas the northeasterly winter monsoon is drier with limited fluvial sediment supply but has a stronger wind and wave regime. Consequently, along the NE-SW trending East Sea coastline, a significant fraction of sediments deposited and stored near the river mouths in summer are reworked in winter and transported southwestwards by the wave-generated longshore current. This is aided by tidal currents^{12,22,29} and there is also a clear sediment segregation. Sandier sediments are dominant from the river mouths to about 30 km downdrift (westward) of the Bassac River mouth, the most westward of the mouths, while further downdrift the coast is composed mainly of mud³⁰ (Fig. 1B). This segregation is also recorded in the relict deltaic landforms as sandy beach ridges only occur in the river mouth area¹⁶, whereas the Camau Peninsula consists almost entirely of a muddy delta plain.

Four shoreline segments (Segs 1–4) in the delta were defined from spatial analysis spanning from 1973 to 2015¹³ (Figs. 1B, C). Seg 1, occurring at the river mouth area from the NE end of the shoreline to 30 km SW of Bac Lieu, showed progradation during most of the interval with decreasing accretion and a switch to erosion between 2010 and 2015. Seg 2, stretching from the SW end of Seg 1 to the tip of the Camau Peninsula at Camau Point, has retreated consistently at a rate > 20 m/year. Seg 3, a complex coastline from Camau Point to an inlet at Song Doc, showed large variations associated with a gradual decrease in the net accretion rate. Seg 4, between Song Doc and Rach Gia, showed the least accretion among the four segments until early 1990 when erosion started to occur. Here, the Seg 1 shoreline is further subdivided into Segs 1a and 1b at the mouth of Bassac River (Fig. 1B).

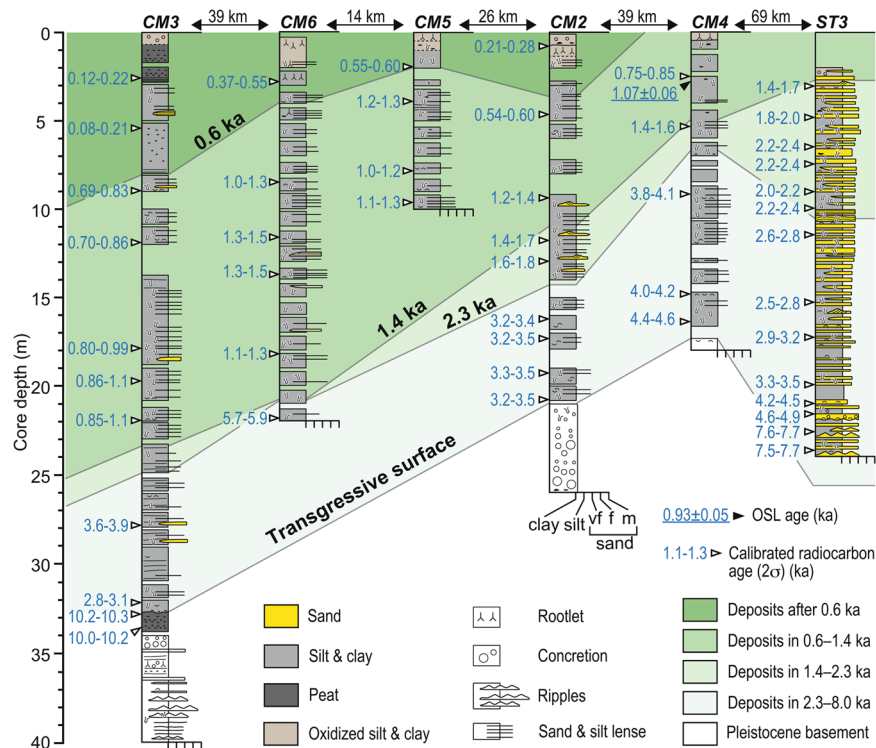


Figure 2. A profile defined by columnar sections of drill cores along the transect X–X' in Fig. 1. Isochrones of 2.3, 1.4, and 0.6 ka are defined according to linear interpolation of radiocarbon ages obtained from Holocene deposits overlying the Pleistocene basement. Core depth is relative to the ground elevation at the individual site.

Results

The sediment cores, full descriptions of which are given in the Supplementary Information, define a cross section through the delta (X–X' in Fig. 1B). Three cores revealed the marine Pleistocene basement sediments beneath the modern delta at depths 17–34 m (Fig. 2). One core (CM3) recorded mangrove sedimentation above this basement during the post-glacial sea-level rise around 10 ka (ten thousand years ago). All other core sediments were deltaic sand and mud with marine mollusc shells and varying degrees of bioturbation. Of note, lateral fining of the sediment facies due to longshore transport was found in core ST3 which exhibited rhythmic alternations of fine to very fine sands and mud, as well as in downdrift cores CM2–6 which showed massive mud intercalated with thin lenses of coarse silt and very fine sand. This corroborates the downdrift segregation identified along the coast and delta front (Fig. 1B).

Radiocarbon and OSL dating provide the chronological framework for events (Figs. 1B and 2). Core ST3 is characterized by continuous accumulation from 4.4 to 1.4 ka. Cores CM2–6 are younger both seawards and downdrift, consistent with the southwestward progradation of the delta. Cores CM2 and CM4 represent sediment accumulation from 4.5 to 3.0 ka, an early stage of the Mekong delta progradation, while all cores record little accumulation for the interval 2.3–1.4 ka. Rapid progradation then occurred after 1.4 ka in cores CM2–6. The upper part of cores CM2, 3, 5 and 6 are dated younger than 0.6 ka, revealing that the shoreline was situated just landward of sites CM2 and CM5 at 0.6 ka. The beach ridges near Soc Trang are dated 1.4–2.8 ka, representing sandy shoreline progradation while offshore sedimentation took place at site ST3 (Fig. 1B). Seaward of Soc Trang beyond a 20-km-wide muddy plain, another beach ridge cluster is dated <0.6 ka. The two beach-ridge sets indicate two phases of slow coastal progradation at 2.8–1.4 ka and after 0.6 ka, between which occurred rapid progradation at 1.4–0.6 ka. OSL ages of intertidal sediments in the muddy plain between Camau city and Vi Thanh range from 0.9 to 2.7 ka and become younger downdrift and seawards, consistent with the shoreline progradation.

Integration of these new and existing data¹⁶ enables, for the first time, reconstruction of isochrones and shoreline positions at 0.6, 1.4, and 2.3 ka along the full stretch of the East Sea coast of the Mekong delta (Fig. 3A). From these we calculated accretion rates for segments 1 and 2 (Fig. 3B). The overall accretion rate of Seg 1 has been consistent over the last 2.3 ka, ranging from +2 to +4 km²/year (except for 1973–77 and after the 1990s). In contrast, Seg 2 shows a drastic increase in the accretion after 1.4 ka, in phase with that of Seg 1b. However, in contrast to Seg 2, after 0.6 ka, accretion of Seg 1b appears to have slowed down whilst that in Seg 2 underwent a dramatic acceleration up to +4 km²/year to form the entire Camau Peninsula. A cartographic analysis¹⁵ has shown that over the period 1885–1940 the eastern 60-km-long fraction of Seg 2 switched to erosion at an average coastal loss rate of –1.5 km²/year. This has evolved into the consistent erosion of the whole Seg 2 at –2–3 km²/year¹³. The total budget of Segs 1 and 2 delta area was slightly positive from the 1970s to 1990s before declined shoreline progradation in Seg 1 caused net shrinkage of the delta. Two important outcomes of the above are that consistent erosion in Seg 2 has been responsible for much of the eroded shoreline in terms of area, and that a drop of c. 6–7

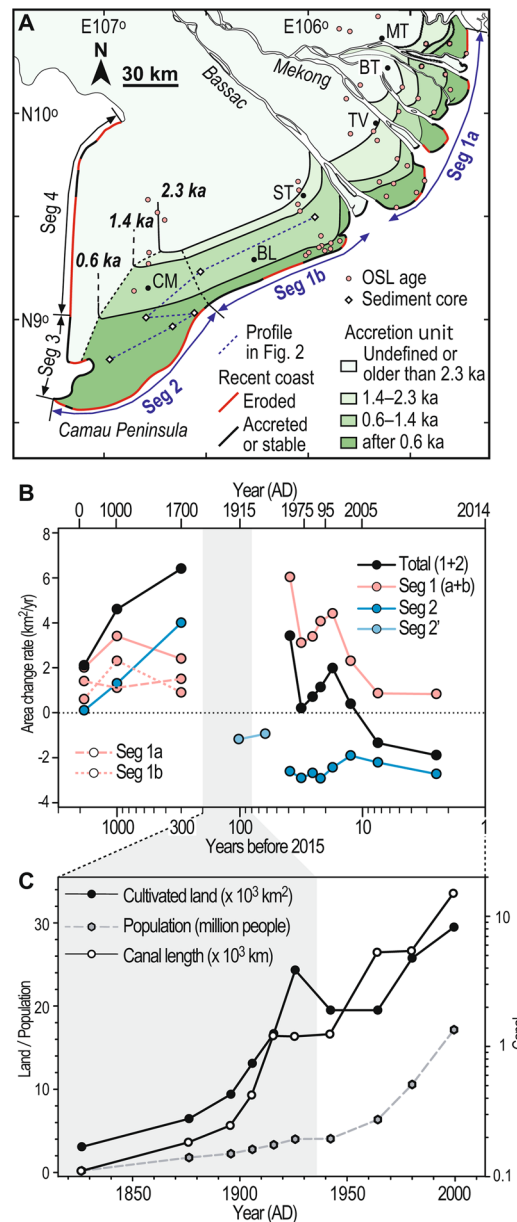


Figure 3. (A) Reconstructed past shorelines of the East Sea coast of the Mekong delta at 2.3, 1.4, and 0.6 ka based on the integration of radiocarbon ages of sediment cores and OSL ages of beach ridges and intertidal mud. ST: Soc Trang, BL: Bac Lieu, CM: Camau, TV: Tra Vinh, BT: Ben Tre, MT: My Tho. Trends of recent shoreline changes are indicated. The map was simplified from Fig. 1B and generated with the software Adobe Illustrator 2020. (B) Estimate of long-term area change rate for shoreline segments defined in Fig. 3A after 2300 years ago along with short-term rates over recent decades^{13,15}. Seg 2' represents the eastern half 60-km-long interval of Seg 2. Rates shown at AD 1913, 1953, 150, 1000, and 1700 represent the average of periods AD 1885–1940, AD 1940–1965, 1.4–2.3 ka, 0.6–1.4 ka, and after 0.6 ka, respectively. Grey shading indicates the period when the canal network was extensively built for irrigation of the Mekong delta under the Vietnamese kingdom and French colonial periods⁴¹. (C) Changes of the cultivated area, population, and total canal length of the Mekong delta over the last 200 years after the existing data compilation⁴³.

km²/year in the sediment budget has occurred sometime before the 1970s relative to the average budget for the last 600 years.

Discussion

The SW coast of the Mekong delta in the East Sea experienced drastic changes in the rate and pattern of progradation over the last 2.5 ka, finally reaching a trend of consistent erosion in the 20th century. Increase in sediment supply after 1.4 ka to Segs 1b and 2 could reflect both an increase in the total muddy sediment load and intensification of longshore transport. This was simultaneous with the enhanced sediment supply to the Chinese rivers by land-use changes in China³¹. These land-use changes are deemed to have accelerated the progradation of the

Red River after 1–2 ka³², and this probably also happened in the neighbouring Mekong's catchment (Fig. 1A). The apparent acceleration of sediment supply after 0.6 ka may also have been favoured by the Chinese population immigration to Yunnan in relation to the Min Dynasty established in the late 14th century. Climate changes, as indicated recently¹⁰, may account for the changes in the sediment discharge. Proxy records in South China³³ and Tibet³⁴ indicate increased regional humidity after 1.5–2 ka. The change in the Mekong delta accretion pattern at 0.6 ka, from uniform progradation of Seg 1b and Seg 2 to selective progradation of Seg 2, indicates sediment bypassing in Seg 1b. This bypassing could be accounted for by intensification of the winter monsoon that drives the longshore transport. Such an intensification has been reported at the onset of the Little Ice Age in East and Southeast Asia³⁵.

Recent dam constructions, fluvial sand mining, and a local decline in mangroves³⁶ cannot account for the current erosion of the eastern coast of the Camau Peninsula and for the correlative erosional features identified in the nearby subaqueous delta³⁰. Our data reveal that the significant decrease in the sediment supply and ensuing erosion likely started between 1885 and 1940. We note that the average recession rate in this period appears similar (c. 20 m/year) to that after the 1970s¹⁵. In contrast to modern recession of the sandy coast, we propose that the causal factor for erosion at this time was sediment sequestration within the deltaic plain due to large-scale anthropogenic modification there. Flood discharge and floodplain inundation have been significantly modified by the construction of a dense network of canals and dikes^{37–40}. This was promoted during the French colonial period from 1858 for navigation and agricultural irrigation^{41,42}. The canal network enabled a drastic increase in the area of rice cultivation on the delta attaining up to 24,000 km² by 1930⁴³ (Fig. 3C). Flood waters were encouraged through the canal network to overflow into rice fields to deposit fertile sediment^{37,44}. This sedimentation, augmented by sediment deposited in the canals, intercepted and stored muddy sediment in the delta plain that would otherwise have been transported to the coast^{40,41}. A mean delta-plain sedimentation rate of 6.86 kg/m² (6 mm/year) has been calculated from field monitoring of a delta area of about 115 km² comprising a dense network of canals³⁹. The normally stagnant water within these fields promotes complete sedimentation of fertile nutrients such that less sediment reaches downstream localities⁴⁰, and, by inference, the coast. If this rate applied to the entire area of rice cultivation by the year 1930, this should have led to a huge decline in coastal mud supply. Whilst the emergence of the canal network impacted on the coastal mud supply, the bedload transported sand in delta distributaries remained unaffected. As a result, the sandy coast corresponding to Seg 1 continued progradation until the 1990s whilst the muddy Seg 2 coast eroded rapidly. It is noteworthy, however, that even Seg 1 has shown signs of a slow-down in progradation since 2003¹². Finally, the hysteresis of longer-term sedimentation also appears to have created conditions that have ultimately favoured coastal erosion. The very rapid progradation of the Camau Peninsula after 0.6 ka enhanced its exposure to waves and longshore currents driven by the winter monsoon winds, and this has led to its increased vulnerability to erosion. This erosion²⁹ can be further exacerbated by aggravated land subsidence notably related to water extraction that drastically increased after the 1990s¹¹ and by ongoing change in sea levels. The extent to which sand mining and consequent deepening of the Mekong delta distributary channels⁶ affect mud redistribution is another issue for further work. Channel deepening may have a possible feedback effect on saline intrusion and re-introduction of mud up-estuary in the dry season that could potentially diminish the amount of mud transported along the eastern coast towards the Camau Peninsula¹². The implications of our study are that even if sediment supply was restored to pre-1990s levels this would be insufficient to prevent further erosion of the Mekong's muddy shorelines.

Methods

To constrain the long-term deltaic sedimentation record and shoreline changes, we obtained six sediment cores, 66 radiocarbon ages, and 13 and 7 optically-stimulated luminescence (OSL) ages for beach-ridge and muddy-plain sediments, respectively. Sediment cores obtained at sites ST3 and CM2–6 (Fig. 1B, Table S1) were halved vertically and described for identification of sediment facies and collection of mollusc shells and plant fragments for radiocarbon dating. Sediment samples for OSL dating were collected by a hand auger at depths of 0.87–2.05 m, except for one taken at 2.6–2.65 m depth in core CM-4. Levels of auger samples correspond to the upper foreshore to basal foredune levels at beach ridge sites and to the intertidal level of the muddy plain, and thus are considered to represent the shoreline deposition. The cumulative subsidence of the sample sites is modeled as <0.3 m¹¹ and thus insignificant. Analytical details of radiocarbon and OSL dating are provided in the supporting information. OSL ages and calibrated radiocarbon ages are expressed relative to AD 2015.

Received: 16 February 2020; Accepted: 20 April 2020;

Published online: 15 May 2020

References

1. Syvitski, J. P. & Saito, Y. Morphodynamics of deltas under the influence of humans. *Glob. Planet. Change* **57**, 261–282 (2007).
2. Giosan, L., Syvitski, J., Constantinescu, S. & Day, J. Climate change: protect the world's deltas. *Nature* **516**, 31–33 (2014).
3. Best, J. Anthropogenic stresses on the world's big rivers. *Nat. Geosci.* **12**, 7–21 (2019).
4. Walling, D. E. The changing sediment load of the Mekong River. *AMBIO* **37**, 150–158 (2008).
5. Kumm, M., Lu, X. X., Wang, J. J. & Varis, O. Basin-wide sediment trapping efficiency of emerging reservoirs along the Mekong. *Geomorphology* **119**, 181–197 (2010).
6. Brunier, G., Anthony, E. J., Goichot, M., Provansal, M. & Dussouillez, P. Recent morphological changes in the Mekong and Bassac river channels, Mekong delta: The marked impact of river-bed mining and implications for delta destabilisation. *Geomorphology* **224**, 177–191 (2014).
7. Bravard, J.-P., Goichot, M. & Galliot, S. Geography of sand and gravel mining in the Lower Mekong River. First survey and impact assessment. *EchoGéo* **26**, 13659, <https://doi.org/10.4000/echogeo.13659> (2013).
8. Jordan, C. *et al.* Sand mining in the Mekong Delta revisited - current scales of local sediment deficits. *Sci. Rep.* **9**, 17823, <https://doi.org/10.1038/s41598-019-53804-z> (2019).

9. Hackney, C. *et al.* River bank instability is induced by unsustainable sand mining in the lower Mekong River. *Nat. Sustain.* **3**, 217–225, <https://doi.org/10.1038/s41893-019-0455-3> (2020).
10. Darby, S. E. *et al.* Fluvial sediment supply to a mega-delta reduced by shifting tropical-cyclone activity. *Nature* **539**, 276–279 (2016).
11. Minderhoud, P. S. J. *et al.* Impacts of 25 years of groundwater extraction on subsidence in the Mekong delta, Vietnam. *Environ. Res. Lett.* **12**, 064006, <https://doi.org/10.1088/1748-9326/aa7146> (2017).
12. Anthony, E. J. *et al.* Linking rapid erosion of the Mekong River delta to human activities. *Sci. Rep.* **5**, 14745, <https://doi.org/10.1038/srep14745> (2015).
13. Li, X., Liu, J. P., Saito, Y. & Nguyen, V. L. Recent evolution of the Mekong Delta and the impacts of dams. *Earth-Sci. Rev.* **175**, 1–17 (2017).
14. Besset, M., Anthony, E. J., Brunier, G. & Dussouillez, P. Shoreline change of the Mekong River delta along the southern part of the South China Sea coast using satellite image analysis (1973–2014). *Géomorphologie: Relief, Processus, Environnement* **22**, 137–146 (2016).
15. Nguyen, V. L., Ta, T. K. O., Tateishi, M. & Kobayashi, I. Coastal variation and saltwater intrusion on the coastal lowlands of the Mekong River Delta, Southern Vietnam. In: *Land-Sea Link in Asia in Proceedings of an international workshop on sediment transport and storage in coastal sea-ocean system* (ed. Saito, Y., Ikehara, K. & Katayama, H.) 212–217 (1999).
16. Tamura, T. *et al.* Origin and evolution of intertributary delta plains; insights from Mekong River delta. *Geology* **40**, 303–306 (2012).
17. Liu, J. P., DeMaster, D. J., Nittrouer, C. A., Eidam, E. F. & Nguyen, T. T. A seismic study of the Mekong subaqueous delta: Proximal versus distal sediment accumulation. *Cont. Shelf Res.* **147**, 197–212 (2017).
18. Zoccarato, C., Minderhoud, P. S. & Teatini, P. The role of sedimentation and natural compaction in a prograding delta: insights from the mega Mekong delta, Vietnam. *Sci. Rep.* **8**, 11437, <https://doi.org/10.1038/s41598-018-29734-7> (2018).
19. Tamura, T. *et al.* Initiation of the Mekong River delta at 8 ka: Evidence from the sedimentary succession in the Cambodian lowland. *Quat. Sci. Rev.* **28**, 327–344 (2009).
20. Tjallingii, R., Stattegger, K., Stocchi, P., Saito, Y. & Wetzel, A. Rapid flooding of the southern Vietnam shelf during the early to mid-Holocene. *Jour. Quat. Sci.* **29**, 581–588 (2014).
21. Ta, T. K. O., Nguyen, V. L., Tateishi, M., Kobayashi, I. & Saito, Y. Holocene delta evolution and depositional models of the Mekong River delta, southern Vietnam in *River Deltas—Concepts, Models, and Examples* (ed. Giosan, L. & Bhattacharya, J. P.) 453–466 (SEPM, 2005).
22. Anthony, E. J. *et al.* Morphodynamics of an eroding beach and foredune in the Mekong River delta: implications for deltaic shoreline change. *Cont. Shelf Res.* **147**, 155–164 (2017).
23. Tamura, T. *et al.* Monsoon-influenced variations in morphology and sediment of a mesotidal beach on the Mekong River delta coast. *Geomorphology* **116**, 11–23 (2010).
24. Nowacki, D. J., Ogston, A. S., Nittrouer, C. A., Fricke, A. T. & Van, P. D. T. Sediment dynamics in the lower Mekong River: Transition from tidal river to estuary. *Jour. Geophys. Res. Oceans* **120**, 6363–6383 (2015).
25. Gugliotta, M. *et al.* Process regime, salinity, morphological, and sedimentary trends along the fluvial to marine transition zone of the mixed-energy Mekong river Delta, Vietnam. *Cont. Shelf Res.* **147**, 7–26 (2017).
26. McLachlan, R. L., Ogston, A. S. & Allison, M. A. Implications of tidally-varying bed stress and intermittent estuarine stratification on fine-sediment dynamics through the Mekong's tidal river to estuarine reach. *Cont. Shelf Res.* **147**, 27–37 (2017).
27. Xue, Z., Liu, J. P., DeMaster, D., Van Nguyen, L. & Ta, T. K. O. Late Holocene evolution of the Mekong subaqueous delta, southern Vietnam. *Mar. Geol.* **269**, 46–60 (2010).
28. Xue, Z., He, R., Liu, J. P. & Warner, J. C. Modeling transport and deposition of the Mekong River sediment. *Cont. Shelf Res.* **37**, 66–78 (2012).
29. Marchesiello, P. *et al.* Erosion of the coastal Mekong delta: assessing natural against man induced processes. *Cont. Shelf Res.* **181**, 72–89 (2019).
30. Unverricht, D. *et al.* Modern sedimentation and morphology of the subaqueous Mekong Delta, Southern Vietnam. *Glob. Planet. Change* **110**, 223–235 (2013).
31. Wang, H. *et al.* Recent changes of sediment flux to the western Pacific Ocean from major rivers in East and Southeast Asia. *Earth-Sci. Rev.* **108**, 80–100 (2011).
32. Tanabe, S. *et al.* Holocene evolution of the Song Hong (Red River) delta system, northern Vietnam. *Sed. Geol.* **187**, 29–61 (2006).
33. Dykoski, C. A. *et al.* A high-resolution, absolute-dated Holocene and deglacial Asian monsoon record from Dongge Cave, China. *Earth Planet. Sci. Lett.* **233**, 71–86 (2005).
34. Bird, B. W. *et al.* Late-Holocene Indian summer monsoon variability revealed from a 3300-year-long lake sediment record from Nirpa Co, southeastern Tibet. *The Holocene* **27**, 541–552 (2017).
35. Tamura, T. *et al.* Luminescence dating of beach ridges for characterizing multi-decadal to centennial deltaic shoreline changes during Late Holocene, Mekong River delta. *Mar. Geol.* **326**, 140–153 (2012).
36. Besset, M. *et al.* Mangroves and shoreline erosion in the Mekong River delta, Viet Nam. *Estuar. Coast. Shelf Sci.* **226**, 106263, <https://doi.org/10.1016/j.ecss.2019.106263> (2019).
37. Hung, N. N. *et al.* Floodplain hydrology of the Mekong Delta Vietnam. *Hydrol. Process.* **26**, 674–686 (2011).
38. Hung, N. N. *et al.* Sedimentation in the floodplains of the Mekong Delta, Vietnam. Part I: suspended sediment dynamics. *Hydrol. Process.* **28**, 3132–3144 (2013).
39. Hung, N. N. *et al.* Sedimentation in the floodplains of the Mekong Delta, Vietnam. Part II: deposition and erosion. *Hydrol. Process.* **28**, 3145–3160 (2013).
40. Kuenzer, C. *et al.* Flood mapping and flood dynamics of the Mekong delta: ENVISAT-ASAR-WSM based time series analyses. *Remote Sens.* **5**, 687–715 (2013).
41. Biggs, D. Canals in the Mekong Delta: a historical overview from 200 C.E. to the present. *Water Encyclopedia* **4**, 748–752 (2005).
42. SIWRP. The project for Climate Change Adaptation for Sustainable Agriculture and Rural Development in the Coastal Mekong Delta in Vietnam – Final Report (Japan International Cooperation Agency, 2013).
43. Nguyen, H. H., Dargusch, P., Moss, P. & Tran, D. B. A review of the drivers of 200 years of wetland degradation in the Mekong Delta of Vietnam. *Reg. Environ. Change* **16**, 2303–2315 (2016).
44. Tran, D. D. & Weger, J. Barriers to implementing irrigation and drainage policies in an Giang Province, Mekong Delta, Vietnam. *Irrigation and Drainage* **67**, 81–95 (2018).
45. Nguyen, V. L., Ta, T. K. O. & Tateishi, M. Late Holocene depositional environments and coastal evolution of the Mekong River Delta, southern Vietnam. *Jour. Asian Earth Sci.* **18**, 427–439 (2000).

Acknowledgements

This project was funded by a Grant-in-Aid for Scientific Research (B) (No. 17H02980) from the Japan Society for the Promotion of Science to Y.S. and the NAFOSTED Vietnam project 105.03-2018.12 to T.K.O.T., as well as by an internal grant of Geological Survey of Japan, AIST. We express thanks to Rob Ashurst, Kana Takamori, and Kazumi Ito for their laboratory assistance. The paper was significantly improved by the journal editor Luigi Tosi and three anonymous reviewers.

Author contributions

T.T. and Y.S. designed the study. T.T., V.L.N., T.K.O.T., M.G., and Y.S. analyzed the sediment cores; R.N. identified species of mollusc shells; T.T. and M.D.B. carried out the OSL dating; T.T. and E.J.A. wrote the manuscript; V.L.N., T.K.O.T., M.D.B., M.G., and Y.S. contributed to the discussion and commented on the manuscript; All authors reviewed and approved the final version of the manuscript.

Competing interests

The authors declare no competing interests.

Additional information

Supplementary information is available for this paper at <https://doi.org/10.1038/s41598-020-64630-z>.

Correspondence and requests for materials should be addressed to T.T.

Reprints and permissions information is available at www.nature.com/reprints.

Publisher's note Springer Nature remains neutral with regard to jurisdictional claims in published maps and institutional affiliations.



Open Access This article is licensed under a Creative Commons Attribution 4.0 International License, which permits use, sharing, adaptation, distribution and reproduction in any medium or format, as long as you give appropriate credit to the original author(s) and the source, provide a link to the Creative Commons license, and indicate if changes were made. The images or other third party material in this article are included in the article's Creative Commons license, unless indicated otherwise in a credit line to the material. If material is not included in the article's Creative Commons license and your intended use is not permitted by statutory regulation or exceeds the permitted use, you will need to obtain permission directly from the copyright holder. To view a copy of this license, visit <http://creativecommons.org/licenses/by/4.0/>.

© The Author(s) 2020